Cellular and Molecular Neurobiology (2019) 39:415–434
https://doi.org/10.1007/s10571-019-00659-7

ORIGINAL RESEARCH

Mammalian Target of Rapamycin 2 (MTOR2) and C-MYC Modulate Glucosamine-6-Phosphate Synthesis in Glioblastoma (GBM) Cells Through Glutamine: Fructose-6-Phosphate Aminotransferase 1 (GFAT1)

Bo Liu[1,2,3] · Ze-Bin Huang[3] · Xin Chen[3] · Yi-Xiang See[3] · Zi-Kai Chen[3] · Huan-Kai Yao[3]

Received: 19 November 2018 / Accepted: 1 February 2019 / Published online: 15 February 2019

Abstract
Glucose and glutamine are two essential ingredients for cell growth. Glycolysis and glutaminolysis can be linked by glutamine: fructose-6-phosphate aminotransferase (GFAT, composed of GFAT1 and GFAT2) that catalyzes the synthesis of glucosamine-6-phosphate and glutamate by using fructose-6-phosphate and glutamine as substrates. The role of mammalian target of rapamycin (MTOR, composed of MTOR1 and MTOR2) in regulating glycolysis has been explored in human cancer cells. However, whether MTOR can interact with GFAT to regulate glucosamine-6-phosphate is poorly understood. In this study, we report that GFAT1 is essential to maintain the malignant features of GBM cells. And MTOR2 rather than MTOR1 plays a robust role in promoting GFAT1 protein activity, and accelerating the progression of glucosamine-6-phosphate synthesis, which is not controlled by the PI3K/AKT signaling. Intriguingly, high level of glucose or glutamine supply promotes MTOR2 protein activity. In turn, up-regulating glycolytic and glutaminolytic metabolisms block MTOR dimerization, enhancing the release of MTOR2 from the MTOR complex. As a transcriptional factor, C-MYC, directly targeted by MTOR2, promotes the relative mRNA expression level of GFAT1. Notably, our data reveal that GFAT1 immunoreactivity is positively correlated with the malignant grades of glioma patients. Kaplan–Meier assay reveals the correlations between patients' 5-year survival and high GFAT1 protein expression. Taken together, we propose that the MTOR2/C-MYC/GFAT1 axis is responsible for the modulation on the crosstalk between glycolysis and glutaminolysis in GBM cells. Under the condition of accelerated glycolytic and/or glutaminolytic metabolisms, the MTOR2/C-MYC/GFAT1 axis will be up-regulated in GBM cells.

Keywords Glycolysis · Glutaminolysis · MTOR2 · GFAT1 · GBM

Background

Cancer cells rely on a variety of metabolic nutrients. And the consumption of specific nutrients used by cancer cells are impacted by both the genetic and environmental context (Cairns et al. 2011a; Cantor and Sabatini 2012; Dang 2012; DeBerardinis et al. 2008, 2010; Levine and Puzio-Kuter 2010). Most mammalian cells use glucose as a fuel source. Glucose is metabolized by glycolysis in a multistep set of reactions, which ultimately results in the generation of pyruvate that enters the mitochondria where it is oxidized by the Krebs Cycle to generate ATP to meet cell's energy demands under normal oxygen condition (Kaelin and Ratcliffe 2008; Koppenol et al. 2011). However, under hypoxic condition, much of pyruvate will be converted into lactate through the

✉ Bo Liu
boliu@umac.mo; lbfhsum@yeah.net

1 Laboratory of Molecular Genetics, University of Maryland School of Medicine, Baltimore 21021, USA

2 Department of Otorhinolaryngology Head & Neck Surgery, University of Maryland School of Medicine, Baltimore 21021, USA

3 Center of Reproduction, development and aging, Institute of Translational Medicine, Cancer Centre, Faculty of Health Sciences, University of Macau, Hengqin 999078, Macau, SAR, China

catalysis of lactate dehydrogenase (LDH/LDHA) outside mitochondria (Lee et al. 2011; Lunt and Vander Heiden 2011; Marroquin et al. 2007; Medina and Núñez de Castro 1990; Pelicano et al. 2006; Qie et al. 2012; Rohle et al. 2013). Lactate production in the presence of oxygen is termed as "aerobic glycolysis" or the "Warburg Effect" (Kaelin and Ratcliffe 2008; Koppenol et al. 2011; Vander Heiden et al. 2009; Warburg 1956). Several signaling pathways are involved in regulating the Warburg Effect in cancer cells. Growth factor stimulation can activate the PI3K/Akt/mTOR cascade that promotes glucose transporter activity and stimulates glycolysis through the activation of several glycolytic enzymes including hexokinase and phosphofructokinase (PFK) (Biggs et al. 1999; Choe et al. 2003; Christofk et al. 2008; Faubert et al. 2013; Gan et al. 2010; Guertin et al. 2006; Hagiwara et al. 2012; Muellner et al. 2011; Plas and Thompson 2005; Tanaka et al. 2011; Wang et al. 2011).

Cancer cells can also use glutamine as another fuel source. Glutamine enters the mitochondria where it can be used to replenish Krebs Cycle intermediates or to produce more pyruvate through the action of malic enzyme (Altman et al. 2016; Cairns et al. 2011b; Cantor and Sabatini 2012; Dang 2012; DeBerardinis et al. 2010; Medina and Núñez de Castro 1990). Glutamine, as an important metabolic fuel, helps cancer cells meet the increased demand for ATP during rapidly proliferative periods (DeBerardinis et al. 2007; Medina and Núñez de Castro 1990; Shanware et al. 2011). Under physiological condition, glutamine enters cells through the amino acid transporter, and will be converted to glutamate in mitochondria through the catalysis of the rate-limiting enzyme glutaminase (GLS). Glutamate will be converted to α-ketoglutarate [α-KG, a critical metabolite that serves in both ATP production and in replenishing the tricarboxylic acid (TCA) cycle intermediates] through the catalysis of glutamate dehydrogenase (GDH; Shanware et al. 2011; Wellen et al. 2010; Wise and Thompson 2010). In addition, glutamate can also be catalyzed by alanine or aspartate transaminases, which promotes the synthesis of a series of amino acids, in addition to α-KG (Tong et al. 2009; Hosios et al. 2016). During the period of hypoxia or mitochondrial dysfunction, α-KG can be converted to citrate in a reductive carboxylation reaction catalyzed by IDH2 (DeBerardinis et al. 2010; Hudson et al. 2002; Kaelin and Ratcliffe 2008; Yang et al. 2016).

The link between glycolysis and glutaminolysis has been deeply investigated in previous studies (Altman et al. 2016; Dang 2012; Le et al. 2012; Levine and Puzio-Kuter 2010; Medina and Núñez de Castro 1990; Qie et al. 2012; Ward and Thompson 2012). However, exact molecular mechanisms underlying the crosstalk between the two metabolic pathways are still poorly understood. Recent studies indicate that rapid proliferating cells, in particular, cancer cells, require the durable supply of both energy and metabolite used as "building blocks." Both glucose and glutamine are consumed to fulfill this requirement (Medina and Núñez de Castro 1990; Qie et al. 2012; Ward and Thompson 2012). As usual, glucose goes through the "aerobic glycolysis" to accelerate the output of lactate. And glutamine is directly transported into the TCA cycle, resulting in the creation of intermediate metabolites, especially citrate, which can be converted to acetyl-CoA as a building block for the synthesis of fatty acids in cancer cells (Le et al. 2012; Marroquin et al. 2007; Shanware et al. 2011).

Glycolysis and glutaminolysis can be linked by hexosamine biosynthesis pathway. And GFAT, the decisive rate-limiting enzyme, is responsible for the regulation of hexosamine biosynthesis in normal and cancer cells. Fructose-6-phosphate and glutamine can be catalyzed to glucosamine-6-phosphate and glutamate that serve as the building blocks for protein and lipid glycosylation in cancer cells through the catalysis of GFAT (DeHaven et al. 2001; Hu et al. 2004; Niimi et al. 2001; Oki et al. 1999). The regulatory role of GFAT in the pathogenesis of diabetes is still under investigation. According to the current studies, it has been reported that GFAT1 is more active in non-insulin-dependent diabetes mellitus patients. Transgenic mice overexpressing this enzyme in skeletal muscle and adipose tissue show an insulin resistance phenotype (DeHaven et al. 2001). In contrast to GFAT1, GFAT2, an isoenzyme of GFAT1, plays a different role in insulin resistance, suggesting its differential regulation on the hexosamine pathway in distinct tissues (Hu et al. 2004; Oki et al. 1999).

Since MTOR2 is considered to be involved in the modulation of both glycolysis and glutaminolysis in cancer cells, we become interested in the molecular link between MTOR2 and GFAT1 in the carcinogenesis of human GBM. Herein, we deeply investigate the roles of the two molecules in regulating glucosamine-6-P synthesis in GBM cells and tissues, and highlight a novel signaling cascade that links the crosstalk between glycolysis and glutaminolysis in GBM cells.

Materials and Methods

Cell Culture

GBM cells (U-118 MG ATCC® HTB-15™) were cultured in Dulbecco's Modified Eagle's Medium (DMEM)/F12 medium (Gibco/Invitrogen, Carlsbad, CA) with L-glutamine, B27 supplement, 1 × solution of penicillin, streptomycin, and fungizone. Cells were maintained at 37 °C in a 5% CO_2-humidified incubator and were subjected to subculture once every 3–4 days. The purity and specificity of cultured cells was confirmed by the immunofluorescent assay of glial fibrillary acidic protein (GFAP), S-100, and Oligo2.

293T cells (ATCC® CRL-1573™) were regularly cultured in DMEM medium (Gibco/Invitrogen, Carlsbad, CA) with L-glutamine, B27 supplement, 1 × solution of penicillin, streptomycin, and fungizone. Cells were maintained at 37 °C in a 5% CO_2 humidified incubator and were subjected to subculture once every 3–4 days.

Colony Formation Assay, Trans-well Chamber Assay, Wound-Healing Assay, In Vivo Metastasis Assay, and Intracranially Implanted Assay

For colony formation assay, 1×10^3 cells were seeded evenly in 6-well plates and medium was changed every 3 days. After 2 weeks, cell colonies were stained by 0.01% crystal violet (Sigma, Japan) and counted.

Cell invasion assay was performed using trans-well chambers (pore size 8 μm, Costar, Corning 3422), with Corning Matrigel Matrix (Corning Incorporated, Corning, NY, USA) for invasion assays. The inserts were placed in 24-well culture plates. Cells were re-suspended in serum-free DMEM medium. Cells (2×10^5 in 200 μl) were added to the upper chamber of Matrigel-coated (for invasion assay) or none Matrigel-coated (for migration assay) membranes with CNF1 (1 nmol/l), LPS, or buffer. 600 μl of medium containing 20% fetal bovine serum with CNF1 (1 nmol/l), LPS, or buffer was added to the lower chamber as a chemoattractant. After 48-h (invasion assay) or 36-h (migration assay) incubation at 37 °C in a 5% CO_2-humidified atmosphere, the cells that had not migrated through the pores were manually removed from the upper face of the filters using cotton swabs, and cells adherent to the bottom surface of the inserts were fixed in 4% paraformaldehyde for 1 h and stained with 0.1% crystal violet (Chemcatch, USA) for 15 min. Finally, the filters were washed three times with PBS and the migrated or invaded cells were stained with crystal violet and images were photographed using a microscope (Leica Microsystems, Germany). In each membrane, the migrated or invaded cell numbers were calculated in 10 randomly selected fields under high-resolution (×40) microscope (Leica Microsystems, Germany).

In wound-healing assay, cells were seeded in 6-well plates and grown until 80–90% confluence. The cells were scratched with a pipette tip in the middle of the plate, washed with PBS to remove the detached cells, and incubated in a medium containing 1% FBS. Cells were treated with 10 mg/ml of mitomycin C for 2 h prior to making the scratch in order to block cellular proliferation. The wound closure was monitored microscopically at different time points and photographed at 0 and 16 h, respectively. The migrated cell numbers were calculated in 10 randomly selected fields under high-resolution (×40) microscope (Leica Microsystems, Germany).

An in vivo xenograft model was established with male BALB/c-nude mice (4–6 weeks, 18–20 g), which were injected subcutaneously with 5×10^6 cells into the right thigh region of the animals ($n = 6$). The tumor weight and volume were evaluated according to the protocol reported in previous study (Wang et al. 2015).

For intracranially implanted assay, U-118 cells were intracranially implanted, using the guide-screw system, into 4- to 6-week-old male nude mice (18–20 g). One week after guide-screw implantation, 500,000 cells were intracranially injected into each mouse brain. A minimum of 10 mice was used in each treatment group to generate survival curves. For in vivo bioluminescent imaging, U-118 Cells were engineered to express luciferase by transducing GSCs with pCignal lenti-CMV-luc viral particles (SABiosciences). Kinetics of tumor growth was monitored by IVIS 200 system bioluminescent imaging. Survival outcomes (100 days post implantation) were estimated using Kaplan–Meier assay.

All animals received human care according to the "Guide for the Care and Use of Laboratory Animals" and the experimental protocols on animals were approved by the Institutional Animal Care and Use Committee at University of Maryland School of Medicine (Baltimore, USA) and University of Macau (Macau, SAR, China). Guidelines for the care and use of animals were followed.

Gene Expression Assay

For miRNA, RNA samples were extracted from the cells treated with TRIzol (Invitrogen). TaqMan miRNA assays (Applied Biosystems) were used to quantify mature miRNA expression. The efficiency of miRNA levels were analyzed by qPCR using Fast SYBR Green Master Mix (Applied Biosystems). For gene knock-down experiments, Lipofectamine RNAiMAX (Invitrogen) was used to transfect siRNAs into cells. For gene over-expression experiments, we used lentivirus vector system. Briefly, the transfer plasmid encoding insert of interest, two packaging plasmids, and envelope plasmid were transfected into 293T cells, and viral supernatant was harvested post culture 48–72 h. Then U-118 cells were infected for 24 h with viral supernatant at MOI 1000, and selection was begun 48 h later with Zeocin (100 mg/ml) (Invitrogen Life Technologies, USA). All adenovirus vectors were purified and amplified using QIAGEN Plasmid maxi kit (Qiagen, Number 12163, Germany). Transfection of plasmids into 293T cells were carried out by ViraPower packaging mix (Invitrogen Life Technologies, USA).

Immunoblotting Assay

Briefly, protein samples extracted from cells or tissues were immersed into RIPA buffer. Protein samples (20.0–100.0 μg) were loaded on Bis–Tris gels (Invitrogen), separated by

SEMS-PAGE, and transferred to nitrocellulose membranes. After 1 h treated in blocking solution (5% non-fat milk in trisbuffered saline, TBS), membranes were incubated with primary antibodies diluted in 5% non-fat milk in TBS/0.1% Tween-20 overnight at 4 °C. After washing with PBS buffer three times, membranes were incubated with horseradish peroxidase-conjugated secondary antibodies for 1 h at 4 °C. Bands were detected by ECL reagents (Invitrogen, USA). The primary antibodies were listed as follows: anti-PI3K p110α antibody (1:1000, Cell Signaling, Danvers, USA), anti-AKT antibody (1:1000, Cell Signaling, Danvers, USA), anti phospho-AKT (Ser473) antibody (1:1000, Cell Signaling, Danvers, USA), anti-MTOR antibody (1:1000, Cell Signaling, Danvers, USA), anti-MTOR2 antibody (1:1000, Cell Signaling, Danvers, USA), anti phospho-MTOR (Ser2448) antibody (1:1000, Cell Signaling, Danvers, USA), anti GFAT1 antibody (1:1000, Cell Signaling, Danvers, USA), anti-beta actin antibody (1:3000, Cell Signaling, Danvers, USA), anti-GAPDH antibody (1:3000, Cell Signaling, Danvers, USA). The corresponding secondary antibodies (1:3000, Cell Signaling, Danvers, USA) were used to react with primary antibodies. The blots were visualized with ECL reagent (Millipore, USA). The band signals were captured by The ChemiDoc MP system (Bio-Rad, CA, USA), and band intensities were measured and analyzed by Image J software (Bio-Rad, CA, USA) according to the protocol provided by company. The ratio of target protein band intensity over GAPDH or β-actin band intensity was calculated by EXCEL software (version, 2007). The final results were presented as mean ± standard deviation (SD) of three independent experiments.

Co-immunoprecipitation assay

Anti-MTOR2 or anti-GFAT1 antibody were coupled to protein G-Sepharose and blocked with BSA. The beads were used to precipitate tagged proteins from cell extracts in RIPA buffer for 1 h at 4 °C. The beads were washed three times with RIPA buffer, boiled in sample buffer, and electrophoresed on an SEMS polyacrylamide gel. After transfer to a PVDF membrane, the bound fraction was assayed for MTOR2 or GFAT1 by immunoblotting using corresponding antibodies, respectively.

Immunohistochemistry

Formalin-fixed, paraffin-embedded tissue sections were cut into 4-μm-thick sequential sections. After deparaffinization and rehydration, sections were boiled in citrate buffer (0.01 M, pH 6.0) for antigen retrieval. Sections were then incubated with 3% H_2O_2 and washed with PBS buffer. 5% goat serum was used to incubate tissue sections for 30 min at room temperature. The sections were then incubated with primary antibody overnight at 4 °C, washed with PBS buffer thrice, and incubated with the corresponding secondary antibody against primary antibody for 1 h at 4 °C. Counterstaining was carried out with hematoxylin. Sections were developed by DAB reagent (Thermo Fisher Scientific, Waltham, Massachusetts, USA). The sections were dehydrated in alcohol and mounted with DPX. Stained sections were observed under light microscope (Zeiss Axioskop). Images were captured with identical exposure settings. The primary antibody: anti-GFAT1 (D9) antibody (1:400, #Sc-377479, Santa Cruz, USA). The corresponding secondary antibody (1:500, Cell Signaling, Danvers, USA) was used to react with primary antibody.

The IHC staining score was based on the staining intensity and percentage positivity (0–100%) of cells in the cytoplasm and nuclei of tumor cells. Four grades were employed: 0, +, ++, and +++. 0 Means no staining, + means faint cytoplasmic and/or nuclei staining in less than 10% positive cells, ++ means moderate cytoplasmic and/or nuclei staining in greater than 10% and less than 50% positive cells, +++ means strong cytoplasmic and/or nuclei staining more than 50% and less than 100% positive cells. In each section, 10 high-resolution (×40) fields were randomly selected and 100 cells in each field were counted under light microscope (Olympus CX43, Japan). The calculation of positive staining cell was monitored by three experienced pathologists (Tiantan Hospital, Beijing, China). In addition, overall staining intensity of GFAT1 was evaluated in the 10 randomly selected fields (×20) of each section by Image-Pro Plus 6.0 software. The final results were presented as mean ± SD of three independent experiments.

Immunofluorescent Assay

Cells were grown on cover slips. Cover slips were rinsed with PBS, then fixed in 100% methanol for 10 min, and washed with PBS. Cover slips were incubated in blocking solution (5% normal goat serum in 0.1% TBS–Tween-20) for 1 h at room temperature and then kept overnight at 4 °C with anti PCNA antibody (1:200, Abcam, Cambridge, Britain), anti BrdU (1:400, Cell Signaling, Danvers, USA), anti C-MYC antibody (1:400, Cell Signaling, Danvers, USA). After rinsing with 0.1% TBS–Tween-20, cells were incubated for 1 h at room temperature with the corresponding secondary antibodies (1:500, Cell Signaling, Danvers, USA) diluted in 4% normal goat serum in TBS. Nuclei was stained by DAPI. Digitized images of signals were obtained with an all-in-one fluorescence microscopy system (Zeiss Axioskop, Germany). Images were captured with identical exposure settings. In each section, 10 high-resolution (×40) fields were randomly selected and observed under fluorescence microscope (BX63, Olympus, Japan). At least 100 cells in

each field were counted under microscope. The final results were obtained from three independent experiments.

Luciferase Activity Assay and ChIP Assay

For Luciferase Activity Assay, pGL3 B vector containing different promoter sequences were transfected into cells. All transfections were performed with Lipofectamine™ 2000 (Invitrogen). After 24-h incubation, luciferase activity was assessed with the Dual-Luciferase Reporter Assay Kit (Promega). For ChIP assay, cells were first cross linked with 1% formaldehyde. Chromatin was prepared from these formaldehyde crosslinked cells and fragmented to an average size of 200–400 bp by sonication. ChIP-Seq experiments were performed by using antibodies against C-MYC (1: 500, Cell Signaling, Danvers, USA). Briefly, 2 µg of the antibodies bound to 20 µl of Dynabeads protein A beads at room temperature for 1 h with rotation. Chromatin mixture was added to the beads + antibody and incubated at 4 °C for overnight with rotation. The immunoprecipitated samples were centrifuged for 1 min at 2000 rpm, and the supernatant was removed. Afterwards, the immunoprecipitated samples were washed by low salt wash buffer, high salt wash buffer and LiCl wash buffer, respectively. The immunoprecipitated samples were subjected to the reversal of cross-link. Afterwards, the purified DNA samples were measured by real-time PCR assay. Then real-time PCR analysis was performed. GFAT1 primers: 5′-GGAATCATCACCAACTAC AAAGAC-3, 5′-AATACTCCACTGCTTTTTCTTCCAC-3.

Clinical Specimens

Fresh tissues (45 tissue samples from glioma patients and 30 tissue samples from craniocerebral trauma patients) were collected from Tiantan Hospital (Beijing, China) from January 2014 to January 2018 for immunoblotting assay of MTOR2, MTOR1, and GFAT1 protein expression levels. All the human tissues were obtained from surgically resected samples from patients. Notably, written informed consent was obtained from all the participants from the Department of Neurosurgery, Tiantan Hospital (Beijing, China). Studies have been approved by Tiantan Hospital (Beijing, China), University of Maryland School of Medicine (Baltimore, USA), and University of Macau (Macau, SAR, China) and National (USA and China) Research Ethics Committee and have been performed in accordance with the ethical standards as laid down in the 1964 Declaration of Helsinki and its later amendments or comparable ethical standards.

Bimolecular Fluorescence Complementation

The bimolecular fluorescence complementation (BiFC) plasmids were obtained from Addgene (pBiFC-VC155/22011 and pBiFC-VN155 (I152L)/27097)35. MTOR coding sequence was cloned into these two vectors according to the available restrictive sites. The principle and specific experimental protocol for BiFC was referenced from Matsui and Lai (2019).

Statistical Assay

The final data shown in figures were presented as mean values and SD of separate experiments ($n \geq 3$). Student's t test was used to compare the differences between two groups. Two-way ANOVA assay was used to compare more than two groups. Survival outcomes were estimated using the Kaplan–Meier method. Statistical calculations were performed using SPSS software (version 19.0, SPSS, Chicago, IL). P value of less than 0.05 ($P < 0.05$) was considered significant.

Results

GFAT1 Maintains the Malignant Features of GBM Cells

To elucidate the role of GFAT1 in GBM cell growth, we employed non-coding RNA technology to knock-down *GFAT1* gene in U-118 cells, and then measured the proliferation abilities of the GFAT1-deficient cells and the control cells. We found that GFAT1 deficiency resulted in the decreased proliferation rates of cells (Fig. 1a–d), implying that GFAT1 played an essential role in promoting GBM cell growth.

In the subsequent study, we evaluated the malignant behaviors of GFAT1-deficient U-118 cells. As expected, GFAT1 deficiency markedly inhibited the migration and invasion abilities of U-118 cells (Figs. 1e–j, 2a, b). And it also limited tumor cell growth and proliferation in an in vivo GBM xenograft model (Fig. 2c–e). To validate this result in mice brains, we generated a GBM intracranial xenograft model. In contrast to control, GFAT1 deficiency impaired the tumor growth and proliferation in brains (Fig. 2f–h). In addition, we observed that GFAT1 deficiency improved the median survival of mice, with median survival prolonged from 76.4 to 96.2 days (Fig. 2g). Overall, these data highlighted the essential role of GFAT1 in maintaining the malignant features of GBM cells.

GFAT1 and MTOR2 Regulate the Synthesis of Glucosamine-6-P in GBM Cells

As shown in Fig. 3a, b, our data revealed that GFAT1 deficiency impaired glucosamine-6-P synthesis in GBM cells, which was accompanied by the reduced glucose

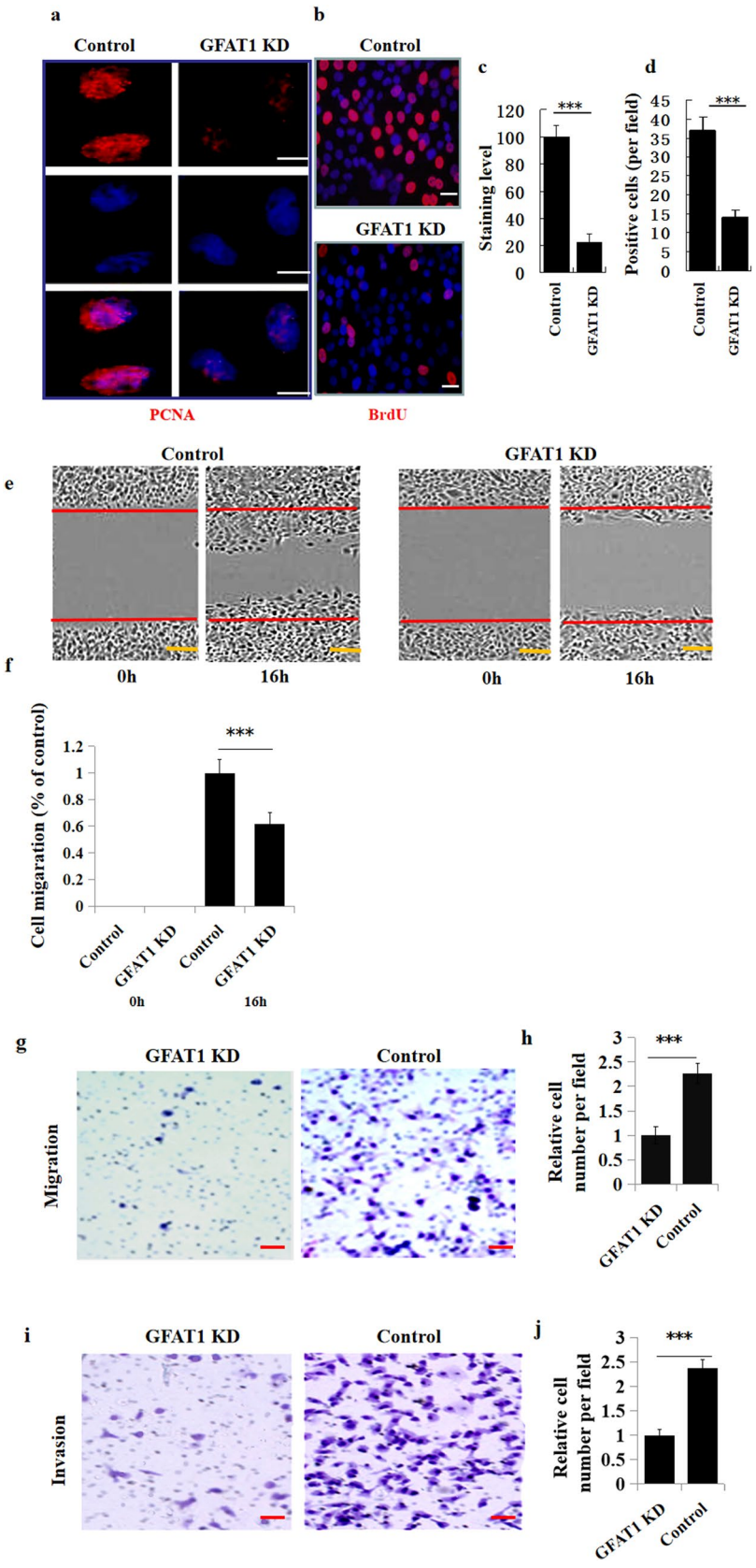

Fig. 1 GFAT1 promotes the proliferation, migration, and invasion of U-118 cells. **a** Immunofluorescent assay of PCNA immunoreactivity. *GFAT1 KD* knock-down of GFAT1 by siRNA. PCNA (red), DAPI (blue). Scale bar = 20 µm. **b** Immunofluorescent assay of BrdU immunoreactivity. BrdU (red), DAPI (blue). Scale bar = 40 µm. **c** Quantitation of PCNA immunoreactivity in the nuclei of U-118 cells. *t* test, $^{***}P < 0.001$. **d** Calculation of BrdU-positive cells. *t* test, $^{***}P < 0.001$. **e** Wound-healing assay. Scale bar = 200 µm. **f** Calculation of cell migration. *t* test, $^{***}P < 0.001$. **g** Trans-well migration assay. Scale bar = 100 µm. **h** Calculation of cell migration. *t* test, $^{***}P < 0.001$. **i** Trans-well invasion assay. Scale bar = 100 µm. **j** Calculation of cell invasion. *t* test, $^{***}P < 0.001$. Bar graphs represent means ± SD of independent experimental triplicates

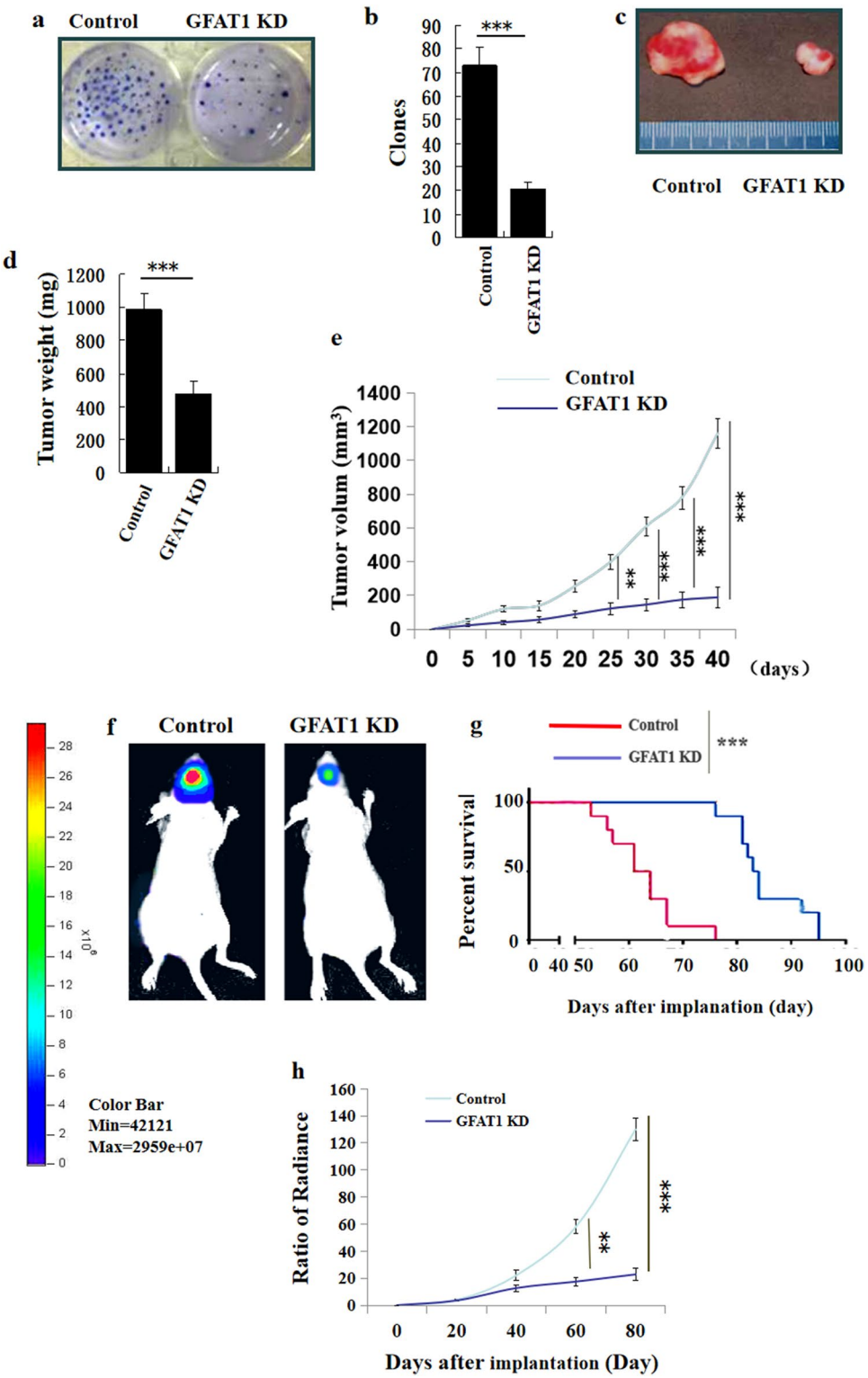

Fig. 2 GFAT1 promotes the metastasis of U-118 cells. **a** Colony assay in soft agar. **b** Calculation of colonies. *t* test, ***$P < 0.001$. **c** Engrafted tumors formed by the GFAT1-deficient U-118 cells and the control cells. **d** Evaluation of the engrafted tumor weights. *t* test, ***$P < 0.001$. **e** Measurements of tumor volumes. ANOVA, **$P < 0.01$, ***$P < 0.001$. **f** Intracranial xenograft assay. **g** Percent survival of mice. Kaplan–Meier assay, ***$P < 0.001$. **h** Ratio of radiance. ANOVA, **$P < 0.01$, ***$P < 0.001$. Bar graphs represent means ± SD of independent experimental triplicates

consumption, glutamine consumption, fructose-6-P synthesis, and glutamate production. To investigate whether MTOR1 and MTOR2 affected glucosamine-6-P synthesis, we used siRNA interference to induce *MTOR1* gene or *MTOR2* gene silence, and measured glucosamine-6-P concentration in U-118 cells. In contrast to MTOR1, MTOR2 deficiency had a profound impact on glucosamine-6-P synthesis in U-118 cells (Fig. 3c–f), implying that MTOR2 rather than MTOR1 played a robust role in regulating glucosamine-6-P synthesis.

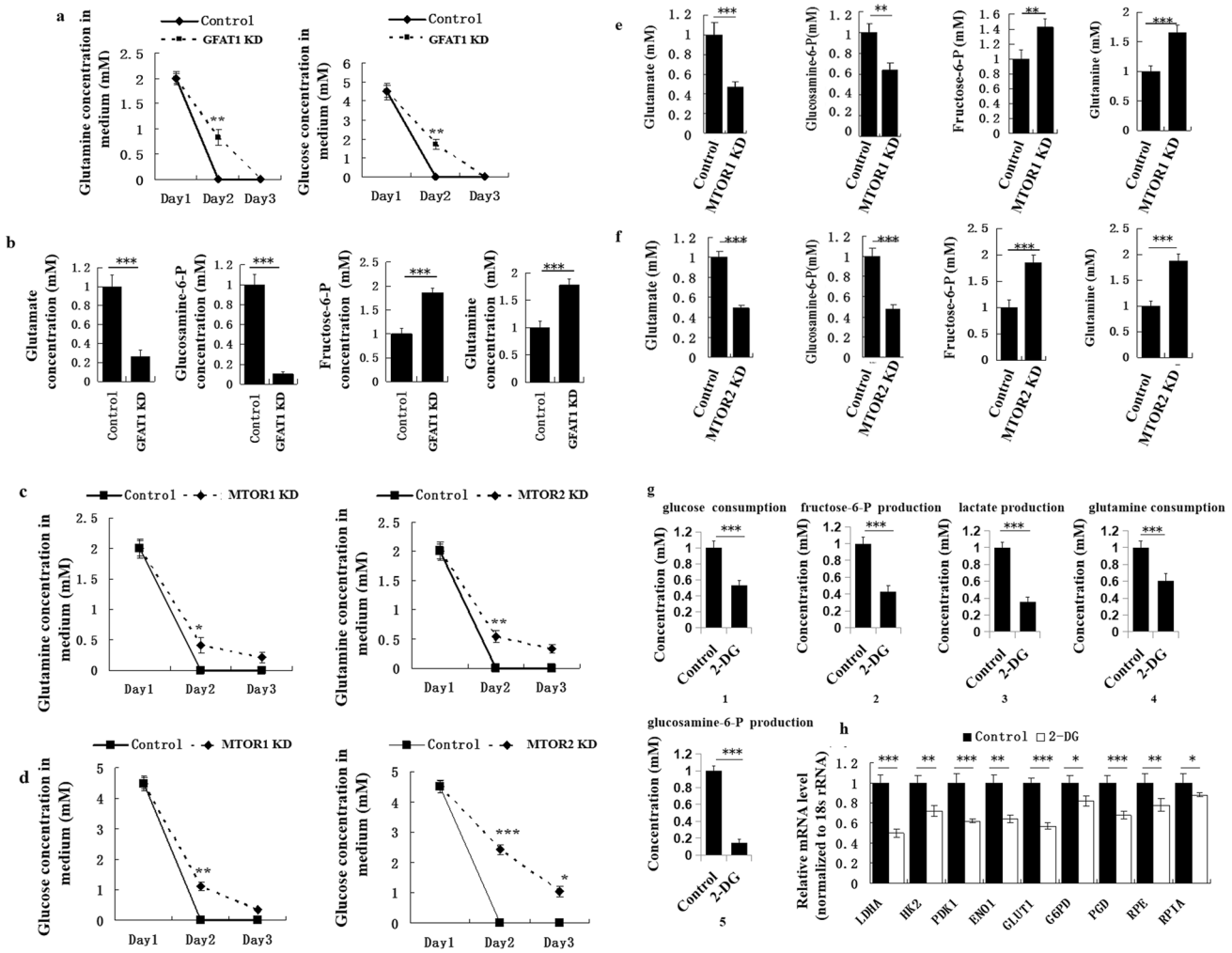

Fig. 3 GFAT1 and MTOR2 promote the glucosamine-P-6 synthesis in U-118 cells. **a** Glutamine concentration measurement in culture medium (left), and glucose concentration measurement in culture medium (right), from culture day 1 to culture day 3. *GFAT1 KD* knock-down of GFAT1 by siRNA. *t* test, $^{**}P<0.01$. **b** Measurements of glutamate, glucosamine-6-P, fructose-6-P and glutamine in U-118 cells. *t* test, $^{***}P<0.001$. **c** Glutamine concentration measurement in U-118 cells. *MTOR1 KD* knock-down of MTOR1 by siRNA, *MTOR2 KD* knock-down of MTOR2 by siRNA. *t* test, $^{*}P<0.05$, $^{**}P<0.01$. **d** Glucose concentration measurement. *t* test, $^{*}P<0.05$, $^{**}P<0.01$, $^{***}P<0.001$. **e** and **f** Measurements of glutamate, glucosamine-6-P, fructose-6-P and glutamine. *t* test, $^{**}P<0.01$, $^{***}P<0.001$. **g** Measurements of glucose consumption (*1*), fructose-6-P production (*2*), lactate secretion (*3*), glutamine consumption (*4*), and glucosamine-6-P production (*5*). *t* test, $^{***}P<0.001$. **h** Real-time RT-PCR assay of relative mRNA levels of the glycolytic enzymes. *t* test, $^{*}P<0.05$, $^{**}P<0.01$, $^{***}P<0.001$. Bar graphs represent means ± SD of independent experimental triplicates

Glucose Concentration Alters MTOR2 and GFAT1 Protein Activities

To investigate the impact of glucose concentration on MTOR2 and GFAT1 protein activity, we applied 2-deoxyglucose (2-DG) (2 mM/l, 48 h) to restrict glycolytic metabolism in U-118 cells. As shown in Fig. 3g, h, relative mRNA levels of the glycolytic enzymes were suppressed in cells, under the condition of blocked glycolytic metabolism. As a consequence of reduced glucose consumption, glutaminolytic metabolism was also suppressed in cells, as indicated by the reduced synthesis of glucosamine-6-P (Fig. 3g). To identify a glucose dose-dependent mechanism by which MTOR2 could regulate glucosamine-6-P synthesis, we examined the protein activities of MTOR2 and GFAT1, in the U-118 cells treated with 2 mM 2-DG and the control cells. As expected, MTOR2 and GFAT1 both displayed the substantially reduced immunoreactivities in cells, under the condition of restricted glucose consumption (Fig. 4a–c). In contrast, high glucose (4.5 g/l) promoted the protein activities of MTOR2 and GFAT1 (Fig. 4a–c), and thereby accelerated the progression of glycolytic metabolism, as indicated by the enhancement of enzymatic activity relevant to glycolysis (Fig. 4d),

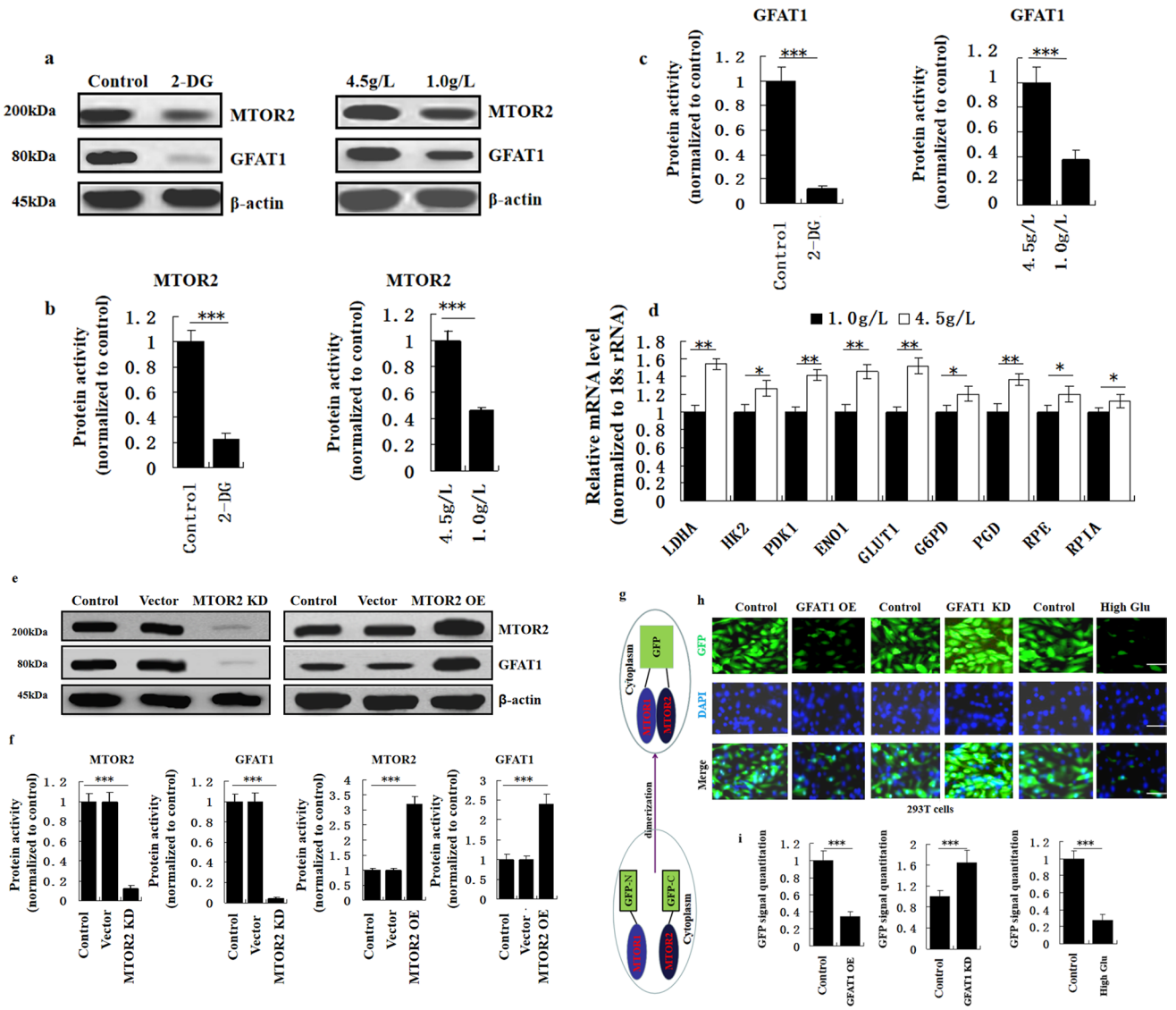

Fig. 4 Glucose concentration alters MTOR2 and GFAT1 protein activities. **a** The effect of restricted glycolytic metabolism (induced by 2 mM 2-DG) (left) and the effect of high glucose concentration (right) on the protein activities of MTOR2 and GFAT1 in U-118 cells. **b** Quantitation of MTOR2 protein activity. *t* test, $***P<0.001$. **c** Quantitation of GFAT1 protein activity. *t* test, $***P<0.001$. **d** Real-time RT-PCR assay of relative mRNA levels of the glycolytic enzymes in U-118 cells. *t* test, $*P<0.05$, $**P<0.01$. **e** Over-expression of MTOR2 or knock-down of MTOR2 altered the protein activity of GFAT1 in U-118 cells. *MTOR2 KD* knock-down of MTOR2 by siRNA, *MTOR2 OE* MTOR2 over-expression. **f** Quantitation of GFAT1 immunoreactivity. *t* test, $***P<0.001$. **g** Schematic illustration of the principle of the bimolecular fluorescence complementation (BiFC) technology. **h** Detection of GFP signals in the cytoplasm of 293T cells by BiFC. Scale Bar: 100 μm. *GFAT1 OE* over-expression of GFAT1, *GFAT1 KD* knock-down of GFAT1 by siRNA, *High Glu* high glutamine. GFP (green), DAPI (blue). **i** Quantitation of GFP intensity. *t* test, $***P<0.001$. Bar graphs represent means ± SD of independent experimental triplicates

implying that MTOR2 and GFAT1 may interact with each other to assist with glycolytic metabolism.

To explore the molecular links between MTOR2 and GFAT1, we used siRNA interference to knock-down *MTOR2* gene, and measured GFAT1 immunoreactivity by Immunoblotting assay. Upon MTOR2 knock-down, GFAT1 immunoreactivity was dramatically suppressed in U-118 cells (Fig. 4e, f). To observe the impact of MTOR2 over-expression on GFAT1 protein activity, we transfected the plasmid vector stably over-expressing MTOR2 and empty vector into U-118 cells, and subsequently measured GFAT1 protein activity. As expected, over-expression of MTOR2 promoted the protein activity of GFAT1 (Fig. 4e, f). Overall, these data demonstrated that MTOR2 enhanced glucosamine-6-P synthesis through up-regulating GFAT1

protein activity, which was controlled by glucose concentration level.

GFAT1, Glucose, and Glutamine Regulate the Dimerization of MTOR1 and MTOR2

We hypothesized that GFAT1 could feedback regulate MTOR2. However, our data suggested that GFAT1 overexpression or deficiency did not alter MTOR2 protein activity (data not shown). In order to investigate whether GFAT1 affected the dimerization of MTOR1 and MTOR2, we employed the BiFC technology. Transfection of both MTOR1-GFP-N and MTOR2-GFP-C constructs into the cytoplasm of 293T cells will generate the intact green fluorescent protein (GFP) via MTOR dimerization. Since MTOR1/2 were expressed in the cytoplasm of cells, the fluorescent signals of GFP-labeled MTOR1/2 could be captured in the cytoplasm of 293T cells. When GFAT1 was over-expressed, the dimerization of MTOR1 and MTOR2 was blocked, as indicated by the weak GFP signal in the cytoplasm of cells (Fig. 4g–i). In contrast, GFAT1 deficiency resulted in the enhanced GFP signal (Fig. 4g–i), implying that GFAT1 negatively regulated the dimerization of MTOR1 and MTOR2 in 293T cells. Upon high glutamine (10 mM/l) stimulation, the dimerization of MTOR1 and MTOR2 was also blocked in the cytoplasm of 293T cells (Fig. 4g–i). Based on these data, we speculated that GFAT1 would promote the release of MTOR2 from the MTOR complex, in order to push the progression of glutaminolysis.

PI3K-AKT Signaling Does Not Alter GFAT1 Protein Activity

Since we had found that GFAT1 could be targeted by MTOR2 in GBM cells, we wondered whether GFAT1 could be controlled by the PI3K-AKT cascade. To solve this problem, we treated U-118 cells with PI3K inhibitor LY294002 (20 μm/l, 48 h). Pharmacological agent could efficiently inhibit the PI3K-AKT signaling. Unexpectedly, this inhibitory effect did not prominently alter GFAT1 protein activity (Fig. 5a, b).

In agreement with the effect of pharmacological treatment, siRNA-mediated PI3K or AKT knock-down could both efficiently inhibit the PI3K-AKT signaling, but not alter GFAT1 protein activity (Fig. 5a, b), implying that MTOR2 could independently regulate GFAT1 activity, which was not monitored by the PI3K-AKT signaling.

To identify the protein–protein interactions between MTOR2 and GFAT1, we performed the co-immunoprecipitation assay. Our data revealed that MTOR2 could directly co-immunoprecipitate with GFAT1 (Fig. 5c). To validate this finding, we used siRNA interference to knock-down *MTOR2* gene or *GFAT1* gene in U-118 cells, and measured the co-immunoprecipitation between the two proteins. Under this condition, we obtained negative results in cells (Fig. 5c). Overall, these data demonstrated that MTOR2 could directly interact with GFAT1 at protein level in GBM cells.

Fig. 5 PI3K-AKT signaling does not alter GFAT1 protein activity in U-118 cells. **a** Immunoblotting assay of protein expression levels of PI3K p110α, AKT, MTOR, p-AKT (S473), p-MTOR (S2448), and GFAT1 in U-118 cells. **b** Quantitation of protein expression levels of PI3K p110α (*1*), AKT (*2*), MTOR (*3*), p-AKT (S473) (*4*), p-MTOR (S2448) (*5*), and GFAT1 (*6*). *t* test, $***P<0.001$. **c** Co-immunoprecipitation assay of the protein–protein interactions between MTOR2 and GFAT1 in U-118 cells. Input was set as positive control. PI (PI material) was set as negative control. **d** Immunoblotting assay of immunoreactivities of MTOR2 and C-MYC in U-118 cells. *MTOR2 KD* knock-down of MTOR2 by siRNA, *MTOR2 OE* MTOR2 over-expression. **e** Immunoblotting assay of immunoreactivities of MTOR2 and C-MYC in U-118 cells. *High Glu* high glutamine. **f** Quantitation of immunoreactivities of MTOR2 and C-MYC. *t* test, $***P<0.001$. *MTOR2 KD* knock-down of MTOR2 by siRNA, *MTOR2 OE* MTOR2 over-expression. **g** Immunoblotting assay of immunoreactivities of nuclear C-MYC and total C-MYC in U-118 cells. *High Glu* high glutamine. **h** Quantitation of nuclear C-MYC immunoreactivity in U-118 cells. *t* test, $***P<0.001$. **i** Immunofluorescent assay of C-MYC immunoreactivity in U-118 cells. Glial fibrillary acidic protein (GFAP, red color), C-MYC (green), DAPI (blue). Scale bar = 100 μm. Arrow points to the location of C-MYC antigen expression. **j** Immunofluorescent assay and quantitation of C-MYC immunoreactivity in the nuclei of the U-118 cells treated with 5.0 or 10 mM/l glutamine (left), and in the nuclei of the U-118 cells treated with 1.0 or 4.5 g/l glucose (right). C-MYC (green), DAPI (blue). Scale bar = 100 μm. *t* test, $***P<0.001$. Bar graphs represent means ± SD of independent experimental triplicates

MTOR2 Positively Regulates C-MYC Protein Activity in GBM Cells

It has been well reported that C-MYC is a critical regulator for cancer cell metabolism, including the Warburg Effect (Dang et al. 2009). Masui et al. reported an unexpected Akt-independent role for MTOR2 in regulating C-MYC level and inducing glycolytic metabolic reprogramming in GBM cells. Consistent with this finding, our data also revealed that MTOR2 positively regulated C-MYC protein activity. Overexpression of MTOR2 promoted C-MYC protein activity. Upon MTOR2 knock-down, C-MYC protein activity was compromised in U-118 cells accordingly (Fig. 5d, f). Under the condition of high glutamine or glucose stimulation, protein activities of MTOR2 and C-MYC were both profoundly enhanced in U-118 cells (Fig. 5e, f). In contrast, restricted glucose consumption, as a consequence of 2 mM/l 2-DG treatment, resulted in the compromised protein expressions of the two proteins (Fig. 5e, f). Notably, increased glucose supply promoted the translocation of C-MYC from nuclei to cytoplasm in U-118 cells (Fig. 5g–j). Similarly, high glutamine supply alleviated the accumulation of C-MYC in the nuclei of U-118 cells (Fig. 5g–j), implying that high

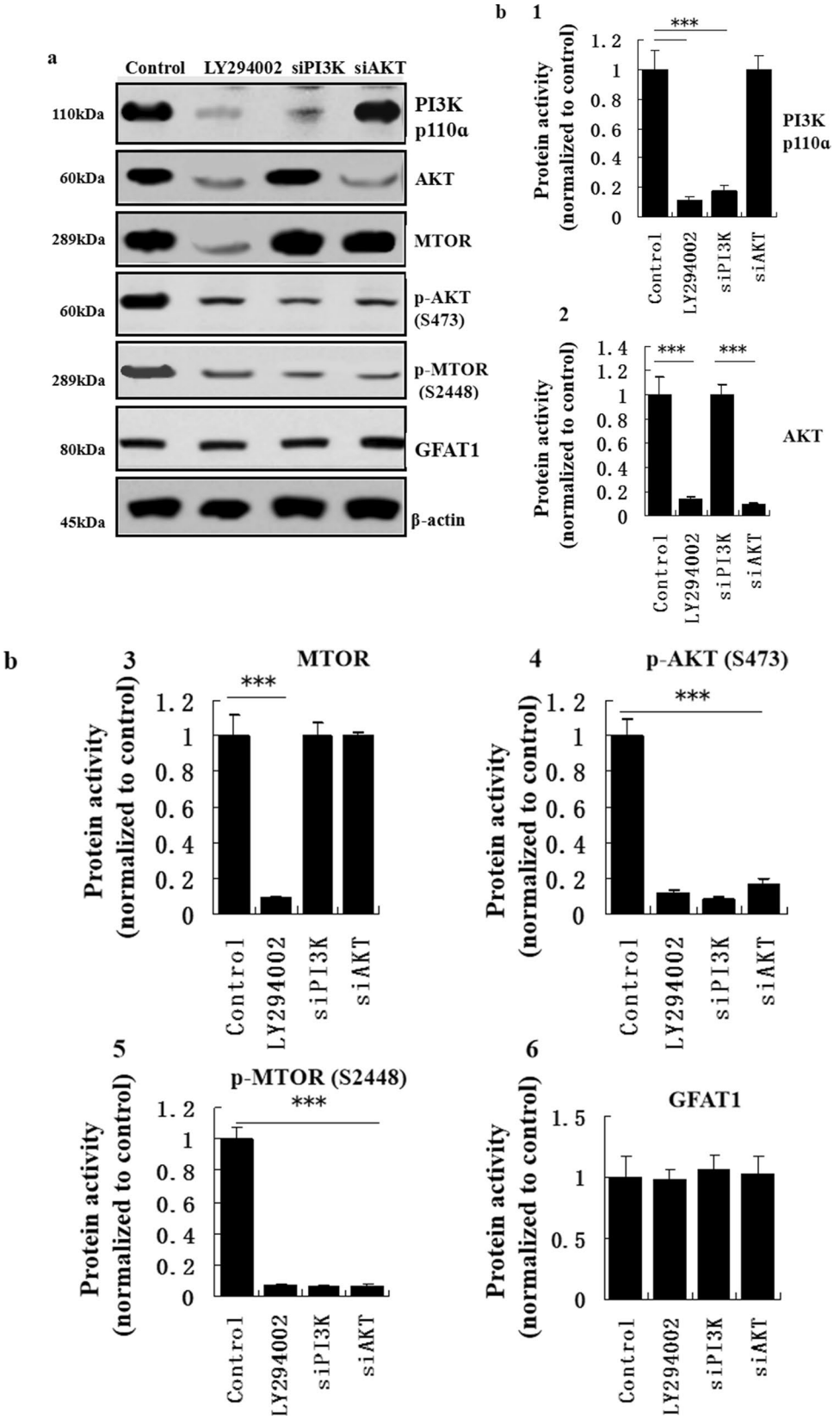
a
Control
LY294002
siPI3K
siAKT
110kDa
PI3K p110α
60kDa
AKT
289kDa
MTOR
60kDa
p-AKT (S473)
289kDa
p-MTOR (S2448)
80kDa
GFAT1
45kDa
β-actin
b
1
Protein activity (normalized to control)
PI3K p110α
2
AKT
3
MTOR
4
p-AKT (S473)
5
p-MTOR (S2448)
6
GFAT1
***
Control
LY294002
siPI3K
siAKT

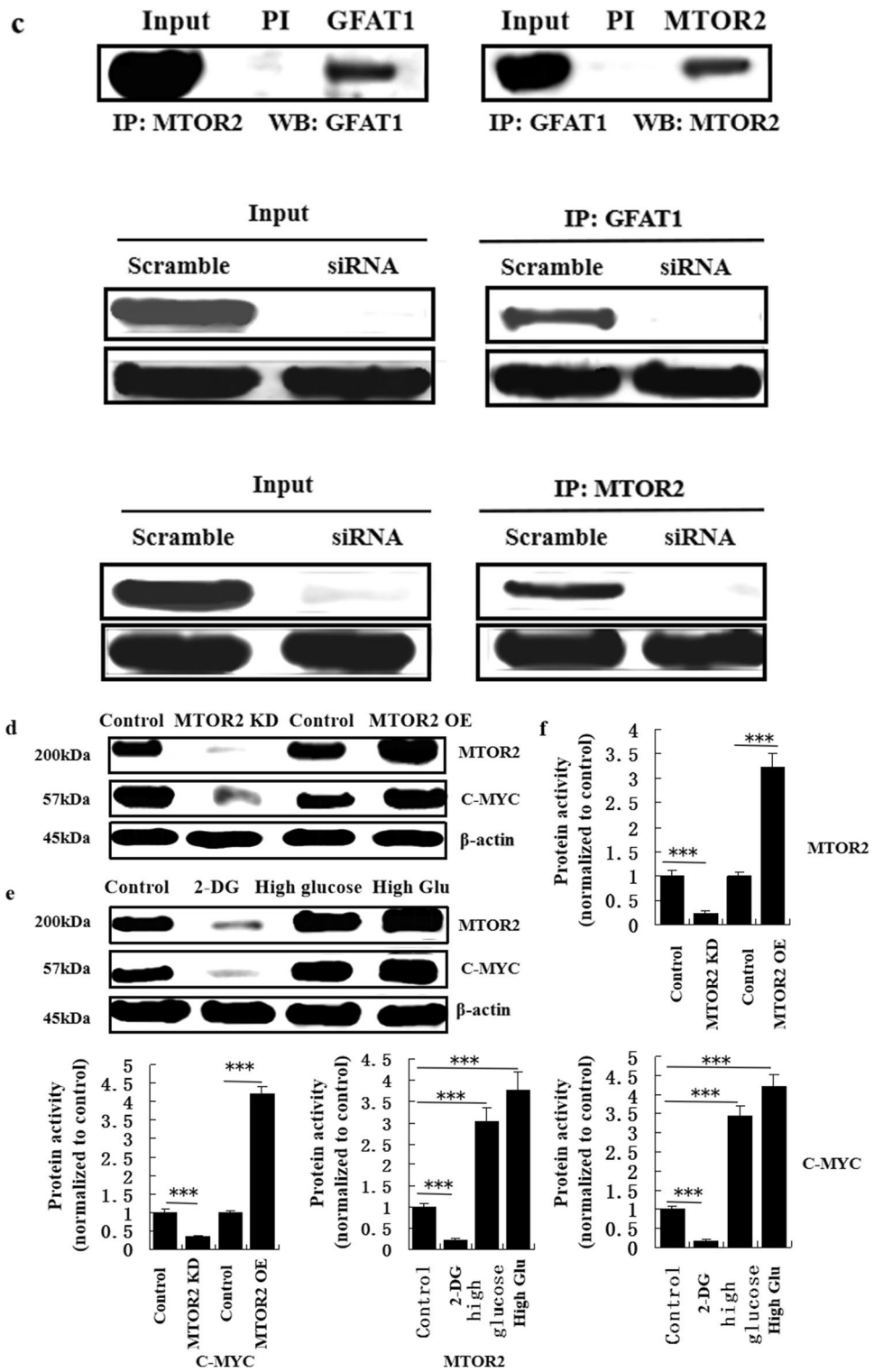

Fig. 5 (continued)

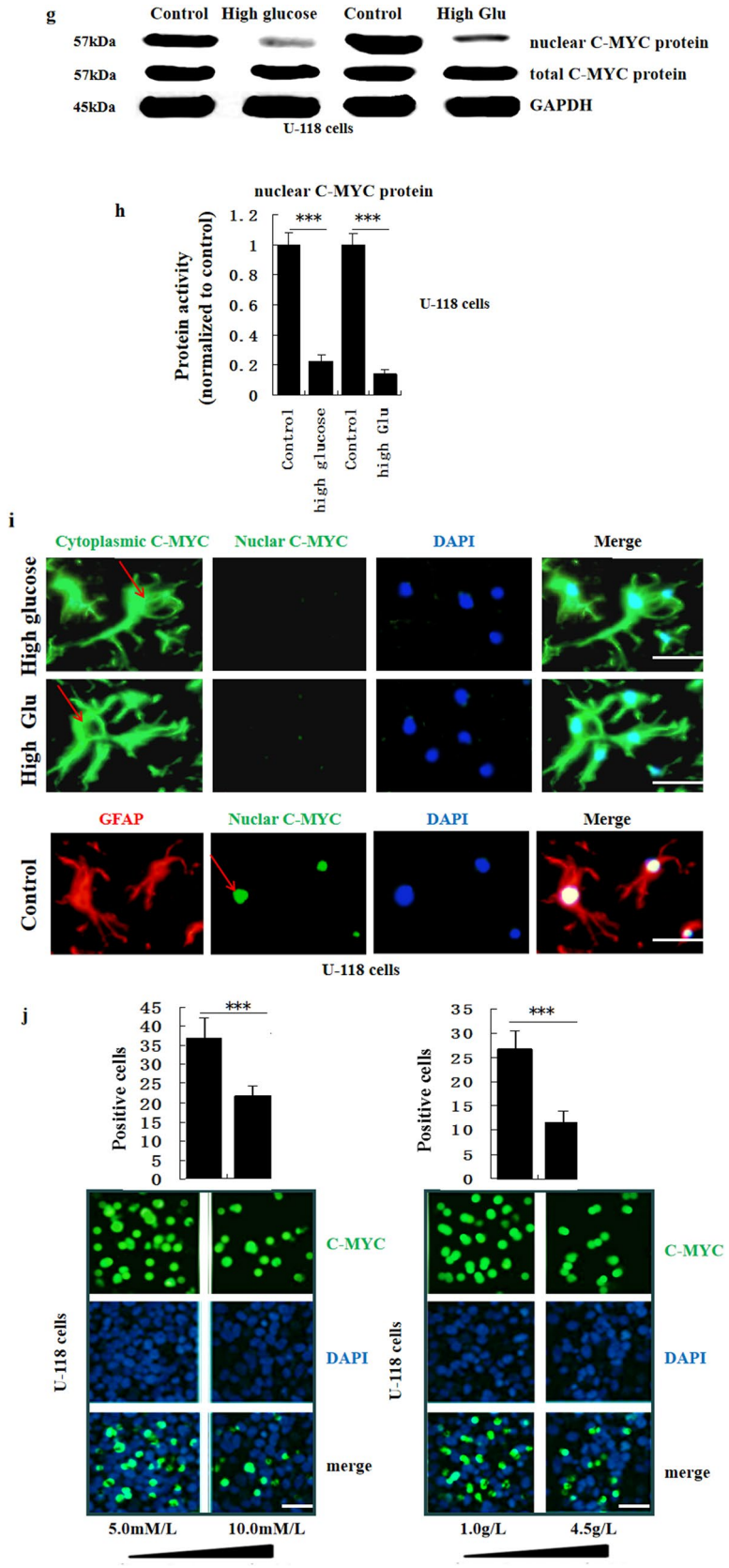

Fig. 5 (continued)

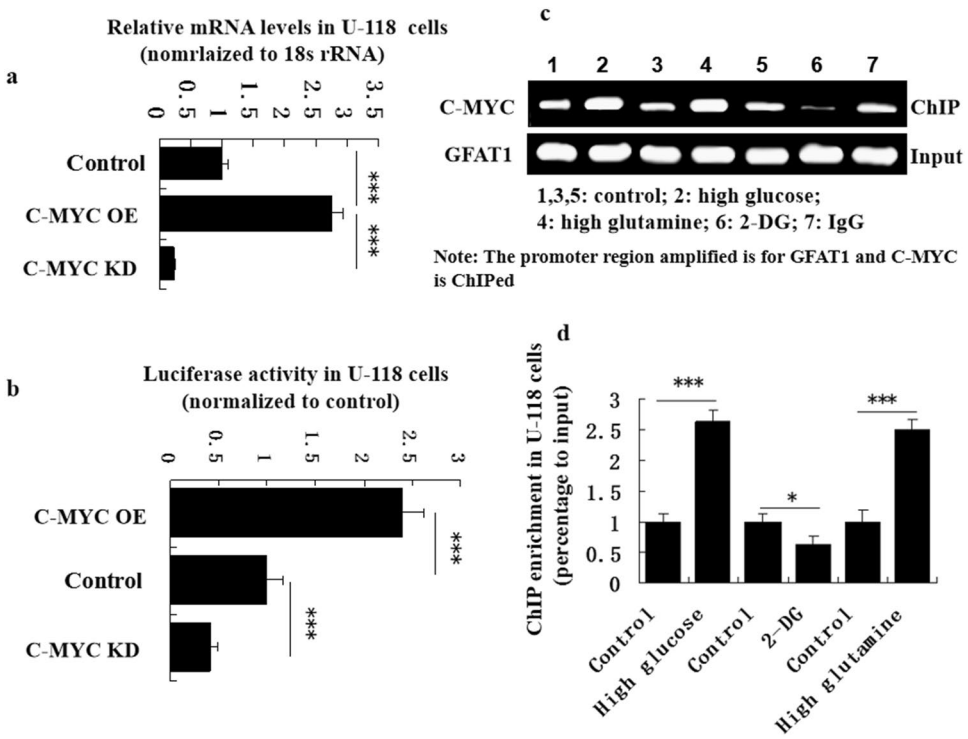

Fig. 6 C-MYC transcriptionally regulates *GFAT1* gene expression in U-118 cells. **a** Real-time RT-PCR assay of relative mRNA expression level of *GFAT1* gene in U-118 cells. *t* test, ***$P < 0.001$. *C-MYC KD* knock-down of C-MYC by siRNA, *C-MYC OE* C-MYC over-expression. *Note* the promoter region amplified is for GFAT1 and C-MYC is ChIPed. **b** Evaluation of luciferase activity in U-118 cells. *t* test, ***$P < 0.001$. **c** ChIP assay of binding activity of C-MYC to *GFAT1* gene promoter in U-118 cells. IgG was loaded as positive control. **d** ChIP enrichment was normalized to input in U-118 cells. *t* test, *$P < 0.05$, ***$P < 0.001$. Bar graphs represent means ± SD of independent experimental triplicates

nutrition supplement would promote the translocation of C-MYC from nuclei to cytoplasm in GBM cells.

C-MYC Transcriptionally Regulates *GFAT1* Gene Expression

To elucidate the role of C-MYC in regulating *GFAT1* gene transcription, we performed the ChIP assay using U-118 cells. As indicated in Fig. 6a, our data revealed that high C-MYC protein level promoted the increased relative mRNA level of GFAT1. To validate this result, we employed the luciferase reporter assay. As shown in Fig. 6b, our data revealed that C-MYC over-expression enhanced the luciferase activity at *GFAT1* promoter in U-118 cells. Upon C-MYC knock-down, luciferase activity at *GFAT1* promoter was reduced accordingly (Fig. 6b). As expected, binding efficiency of C-MYC to *GFAT1* promoter was improved in U-118 cells, in the context of high glucose or high glutamine supply in culture medium (Fig. 6c, d). In contrast, restricted glycolytic metabolism, resulting from 2 mM/l 2-DG treatment, suppressed the binding efficiency of C-MYC to *GFAT1* promoter in U-118 cells (Fig. 6c, d). Overall, these results highlighted the transcriptionally regulatory role of C-MYC in *GFAT1* gene expression in GBM cells. Glucose and glutamine supplements would impact the regulation of C-MYC on *GFAT1* transcription.

Antigen Expression Level of GFAT1 in Glioma Patients' Tissues

To probe for the unattended function of GFAT1 in human glioma tissues, we collected 45 glioma samples (grade I: 8, grade II: 10, grade III: 12, grade IV: 15) and 30 normal brain samples (adjacent to craniocerebral injury tissues). According to the WHO criteria, human glioma can be subdivided into four grades based on its malignancy. Pilocytic astrocytoma is defined as grade I diffuse astrocytoma is defined as grade II, anaplastic astrocytoma is defined as grade III, and GBM is defined as grade IV.

The clinical information including age (average age for glioma patient 46.3, average age for control patient 38.7), gender (glioma group man 34, woman 11, control group man 24, woman 6), pathological grades (grade I: 6, grade II: 17, grade III: 10, and grade IV: 12), tissue origins (astrocytoma 30, oligodendroglioma 12, ependymoma 3), and 5-year survival rate (above 50% for grades I to II, less 20% for grades III to IV) were systematically analyzed by statistical assays.

As shown in Fig. 7a, protein activities of glutamine and glucosamine-6-P were both highly elevated in glioma tissues relative to normal brain tissues. As the enhancement of malignancy, protein activities of the two molecules were elevated accordingly. Immunoblotting assay revealed that MTOR2, MTOR1, and GFAT1 all displayed the substantially enhanced immunoreactivities in glioma tissues. Interestingly, they displayed the highest immunoreactivities in

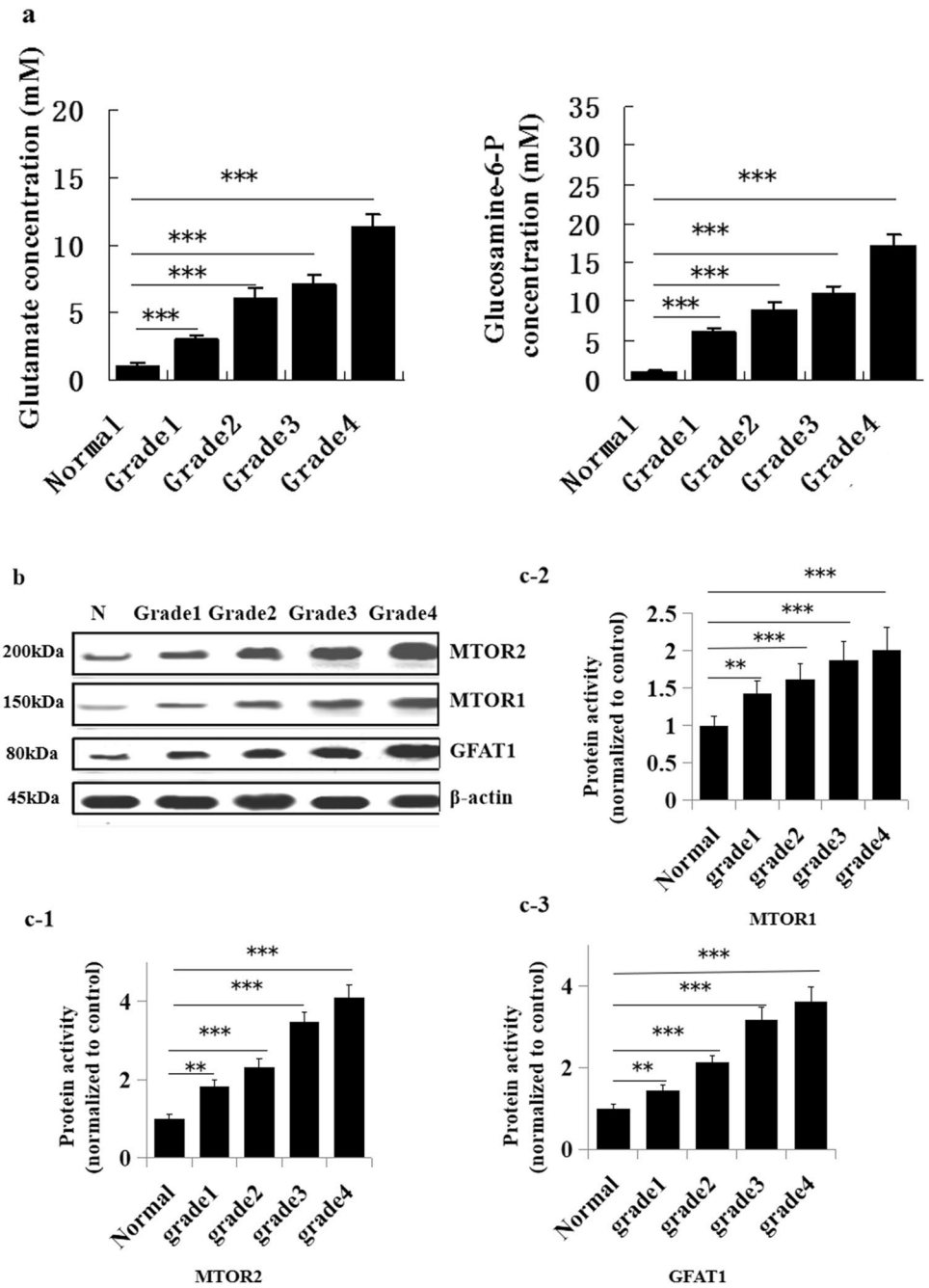

Fig. 7 Elevated protein levels of MTOR2 and GFAT1 in human glioma tissues. **a** Glutamine concentration measurement (left) and glucosamine-6-P concentration measurement (right) in normal brain tissues and glioma tissues. *t* test, $^{***}P<0.001$. **b** Immunoblotting assay of protein activities of MTOR2, MTOR1, and GFAT1 in normal brain tissues and glioma tissues. **c** Quantitation of protein activities of MTOR2, MTOR1, and GFAT1. *t* test, $^{**}P<0.01$, $^{***}P<0.001$. **d** Immunohistochemical assay of GFAT1 antigen expression level in normal brain tissues and glioma tissues. *1* Normal brain, *2* grade I, *3* grade II, *4* grade III, *5* grade IV (GBM). DAB staining. Scale bar = 100 μm (1–4) and 50 μm (5). **e** Evaluation of GFAT1 staining intensity. *t* test, $^{***}P<0.001$. **f** Kaplan–Meier survival assay indicates a correlation between high GFAT1 protein expression and patients' 5-year survival rates. $^{*}P<0.05$. **g** Schematic illustration of crosstalk between glycolysis and glutaminolysis regulated by MTOR2, C-MYC, and GFAT1 in GBM cells. Bar graphs represent means ± SD of independent experimental triplicates

GBM tissues (Fig. 7b, c). In contrast to MTOR1, MTOR2 displayed higher immunoreactivity in glioma tissues (Fig. 7b, c).

To observe GFAT1 immunoreactivity in situ, we conducted the immunohistochemical assay of GFAT1 on glioma tissue sections and normal brain tissue sections, respectively. Digitally scored positive staining cell numbers were divided into four levels: 0 (no positive stained cells), + (0–10% of positive stained cells), ++ (10–50% of positive stained cells), and +++ (50–100% of positive stained cells). Antigen expression of GFAT1 displayed moderate levels (+−++) in normal brain tissues. However, it displayed strong levels (+++) in glioma tissues (Fig. 7d). In addition, GFAT1 staining intensity was gradually elevated in the distinct malignant glioma tissues, and it displayed the strongest level in GBM tissues (Fig. 7e).

Spearman assay revealed that GFAT1 immunoreactivity was positively correlated with the grades of glioma malignancy (r_s=0.601, P=0.0073). However, it was not found to be positively correlated with age, gender, location, and tissue origins. Subsequently, we measured the correlations between patients' survival rates and high GFAT1 protein expression

Fig. 7 (continued)

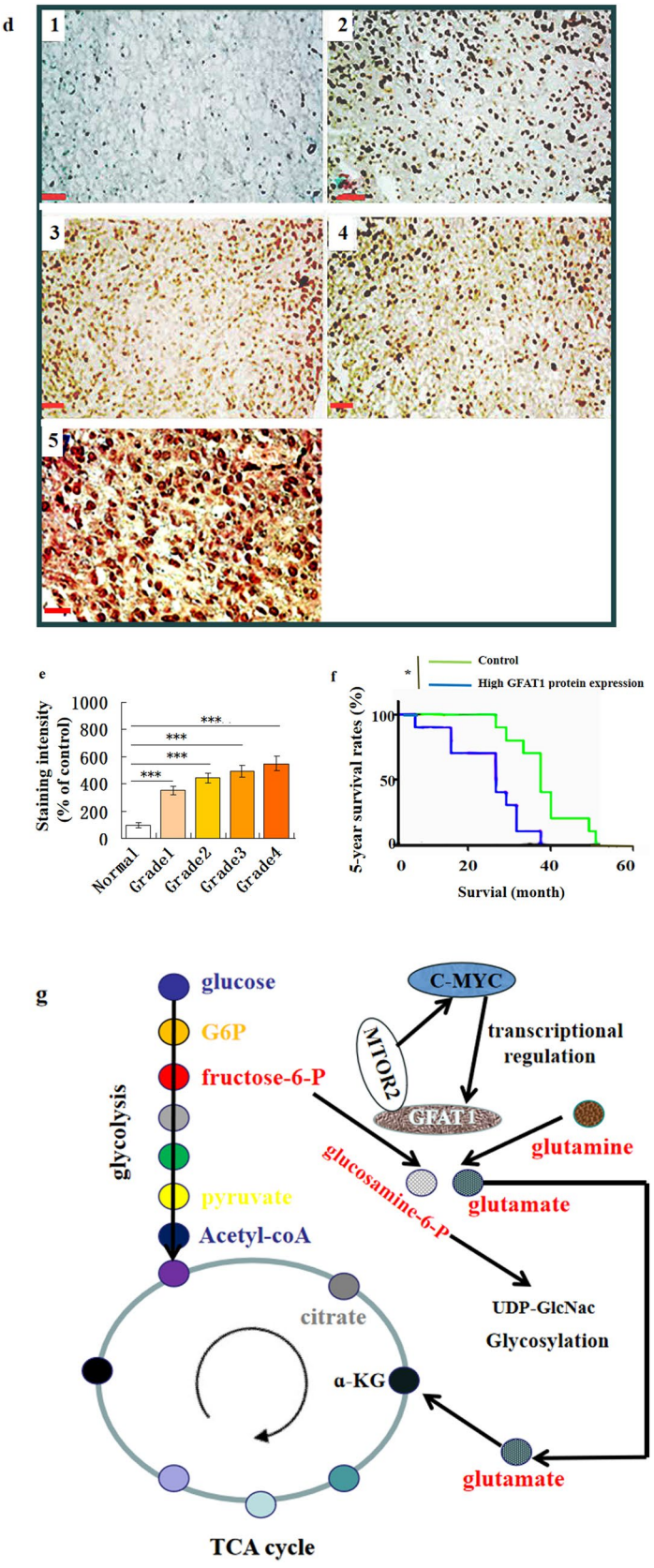

level. Kaplan–Meier analysis indicated that patients' 5-year survival rates decreased dramatically, as the enhancement of GFAT1 immunoreactivity ($P = 0.019$, Fig. 7f). Overall, these data highlighted that GFAT1 could predict the poor prognosis for glioma patients in clinical medicine.

Discussion

In traditional view, glucose and glutamine that can be consumed by cancer cells through distinct metabolic pathways are critical nutrients indispensable for cancer cell growth, proliferation, migration, invasion, and metastasis (Cairns et al. 2011a; Cantor and Sabatini 2012; Dang 2012; DeBerardinis et al. 2008, 2010; DeHaven et al. 2001; Levine and Puzio-Kuter 2010; Muellner et al. 2011; Oki et al. 1999; Vadla and Haldar 2018; Wise et al. 2008; Wise and Thompson 2010; Yang et al. 2016). Usually, glucose is transported into cells and further metabolized to pyruvate that either enters the mitochondria for TCA cycle or will be converted to lactate that also functions as a major advantage nutrient for cancer cell growth (Lee et al. 2011; Lunt and Vander Heiden 2011; Marroquin et al. 2007; Medina and Núñez de Castro 1990; Pelicano et al. 2006; Qie et al. 2012; Rohle et al. 2013). Glutamine, the most abundant amino acid in plasma, positively promotes cancer cell proliferation through the glutaminolysis pathway. During this process, glutamine will be converted into glutamate, which is accompanied by the synthesis of carbon and nitrogen that are essential ingredients for cancer cell growth (Medina and Núñez de Castro 1990; Qie et al. 2012; Ward and Thompson 2012). However, few studies indicate that it is the non-glutamine amino acid, especially aspartate, acting as the critical rate-limiting element and having a critical role in cancer cell proliferation (Hosios et al. 2016).

It has been well reported that MTOR, a highly evolutionarily conserved serine/threonine kinase, positively regulates cellular growth and proliferation in human cancer cells, in response to both extracellular and intracellular signals. It is known that MTOR complex consists of MTOR1 and MTOR2 that mediate separate but overlapping cellular functions. In traditional view, MTORC1 contains three core proteins, MTOR, raptor, and mLST8. The three protein components are responsible for cell growth and proliferation. Raptor is a regulatory protein associated with MTOR that facilitates recruitment of MTOR1 substrates, including ribosomal protein S6 kinase (S6K) and eukaryotic translation initiation factor 4E binding proteins (4E-BPs), for phosphorylation. In contrast to MTOR1, MTOR2 contains mLST8 and rictor (rapamycin-insensitive companion of MTOR) that is an especially critical adapter protein for MTOR2 and can phosphorylate Akt at Ser473 (Christofk et al. 2008; Faubert et al. 2013; Gan et al. 2010; Guertin et al. 2006; Hagiwara et al. 2012; Muellner et al. 2011; Plas and Thompson 2005; Tanaka et al. 2011; Wang et al. 2011).

It has been well reported that MTOR2, the substrate of the PI3K-AKT cascade, is responsible for carcinogenesis in a lot of cell types. A series of growth factors and nutrients can activate the kinase activity of MTOR2, promoting the growth, invasion, and metastasis of a lot of solid tumors. Several studies have reported that MTOR2 can induce tumor cell growth by promoting protein synthesis. In addition, MTOR2 has been found to be involved in the modulation of glycolytic and oxidative metabolism in a lot of human tumor types (Biggs et al. 1999; Choe et al. 2003; Christofk et al. 2008; Faubert et al. 2013; Gan et al. 2010; Guertin et al. 2006; Hagiwara et al. 2012; Muellner et al. 2011; Plas and Thompson 2005; Tanaka et al. 2011; Wang et al. 2011).

We hypothesized that MTOR2 and GFAT1 could be expected to be functionally related in cancer cells; therefore, in this study, we investigated the regulatory roles of MTOR2 and GFAT1 in the crosstalk between glycolysis and glutaminolysis in GBM cells. According to previous studies, fructose-6-P, the intermediate product of glycolysis, together with glutamine, will be converted into glucosamine-6-P through the catalysis of GFAT (Hu et al. 2004; Niimi et al. 2001). Our data report that GFAT1 deficiency profoundly inhibits the proliferation, migration, invasion, and metastasis of GBM cells in vitro, implying that GFAT1 plays an essential role in maintaining the malignant features of GBM cells. In addition, data obtained from human glioma tissues samples also indicated that GFAT1 immunoreactivity was positively correlated with the malignant grades of GBM. Survival assay revealed the correlations between patients' 5-year survival and high GFAT1 protein expression level.

Although it has been reported that MTOR controls cell growth and proliferation and plays a critical role in metabolic reprogramming in human glioma (Tanaka et al. 2011; Wang et al. 2011), we wondered whether MTOR1 and MTOR2 played the distinct roles in regulating glucosamine-6-P synthesis. Intriguingly, our data reveal that MTOR2 rather than MTOR1 plays a robust role in regulating glucosamine-6-P synthesis in GBM cells. Subsequently, our data indicate that MTOR2 and GFAT1 are identified to be functionally related in GBM cells, implying that MTOR2 can regulate glucosamine-6-P synthesis through altering GFAT1 enzymatic activity. Although MTOR1 can be targeted by the PI3K-AKT cascade, our data reveal that MTOR2 is capable of independently regulating the protein activity of GFAT1 in GBM cells, which is not controlled by the PI3K-AKT signaling.

Based on the above descriptions, we consider that MTOR1 may not mainly responsible for glycolytic and glutaminolytic metabolism in GBM cells. Although the molecular mechanism underlying this phenomenon is still obscure, one study has reported that histone H3 lysine 56 acetylation can be efficiently regulated by MTOR2 in GBM cells. Global

histone H3 lysine 56 acetylation levels are down-regulated in the MTOR2-deficient, but not the MTOR1-deficient GBM cells (Vadla and Haldar 2018). In addition, this study has also reported that MTOR2 regulates the expression of the genes responsible for glycolysis by affecting histone H3 lysine 56 acetylation levels at the promoters of these genes in glioma cells. Depletion of MTOR2 leads to the increased recruitment of sirtuin6 (SIRT6) to the promoters of these glycolytic-associated genes (Vadla and Haldar 2018). This molecular mechanism can explain why MTOR2 rather than MTOR1 plays a robust role in regulating the crosstalk between glycolysis and glutaminolysis in GBM cells. The exact role of MTOR1 in the carcinogenesis of GBM cells will be further investigated in the future study. Currently, we consider that MTOR1 is not mainly responsible for regulating energy metabolism in GBM cells.

As a transcription factor, C-MYC is considered to be important in the regulation of both glutamine and glucose metabolism in human cancer types (Wise et al. 2008). Cells over-expressing C-MYC are glutamine-addicted. And increased glutaminase 1 (GLS1) level can be detected in these cells (Gao et al. 2009). And C-MYC promotes the expression of glutamine transporters, enhancing the entry of glutamine into cells, and it strongly supports HIF-1α function by enhancing the enzymatic activities of phosphofructokinase1 (PFK1), phosphofructokinase2 (PKM2), and LDH, ultimately contributing to the enhancement of glycolytic metabolism (Gao et al. 2009; Wise et al. 2008). It has been revealed that C-MYC plays a vital role in the regulation of glycolytic and glutaminolytic enzyme activities in head and neck carcinoma cells (HNSCCs), suggesting that C-MYC inhibitors such as 2-deoxyglucose (2-DG) may play an anti-proliferative role in HNSCCs (Kleszcz et al. 2018). In this study, our data also reveal that 2-DG can efficiently inhibit the progression of glycolytic and glutaminolytic metabolisms in GBM cells, which is accompanied by the reduced protein activities of MTOR2 and C-MYC.

In addition, our study first indicates that C-MYC, directly targeted by MTOR2, is actively involved in the modulation of the link between glycolysis and glutaminolysis in GBM cells. As a transcriptional factor, C-MYC regulates the transcriptional activity of GFAT1 that is responsible for enzymatic activity relevant to both glycolytic and glutaminolytic metabolisms. Intriguingly, high nutrition supplement promotes the translocation of C-MYC from nuclei to cytoplasm in GBM cells. We analyze that C-MYC will interact with GFAT1 in cytoplasm, which results in the enhancement of *GFAT1* gene transcription, ultimately promoting the glucosamine-6-P synthesis in GBM cells.

The regulatory role of GFAT in the pathogenesis of diabetes is still under investigation. It has been reported that GFAT1 and GFAT2 play distinct roles in regulating the development of diabetes. Transgenic mice over-expressing GFAT1 in skeletal muscle and adipose tissue show an insulin resistance phenotype (DeHaven et al. 2001). However, GFAT2 plays a different role in insulin resistance, suggesting its differential regulation on the hexosamine pathway in distinct tissues (Hu et al. 2004; Oki et al. 1999). One research group (Vyas et al. 2013) once developed a combination of pharmacophore modelling, homology modelling, and molecular docking analysis system, which promoted the design of glutamine competitive inhibitors of human GFAT. Based on the descriptions above, we consider that pharmacological agent against GFAT1 or GFAT2 owns the potential to treat diabetes in clinical medicine. In the future study, we will investigate the function of GFAT1/2 inhibitor on the crosstalk between glycolytic and glutaminolytic metabolisms in GBM cells.

Conclusions

We find that GFAT1 is essential to maintain the malignant features of human GBM cells. Our data reveal that MTOR2 and C-MYC cooperatively regulate glucosamine-6-P synthesis through GFAT1, which is not controlled by the PI3K-AKT cascade. And we report that GFAT1 antigen expression level predicts the poor prognosis for glioma patients in clinical medicine. In summary, we propose that the MTOR2/C-MYC/GFAT1 axis plays a vital role in regulating the crosstalk between glycolytic and glutaminolytic metabolisms in GBM cells (Fig. 7g).

Acknowledgements We thank Dr. Qi Zhang (Tiantan Hospital, Beijing, China) for kindly collecting glioma tissue samples and clinical information. This research was funded by the Postdoctoral Research Foundation (2014) provided by the University of Macau, SAR, China.

Author Contributions B.L. designed the research project, performed most of the experiments, analyzed the data, and wrote the manuscript. Z.B.H, X.C., Y.X.S., Z.K.C., and H.K.Y. performed the experiments and analyzed the data.

Compliance with Ethical Standards

Conflict of interest The authors declare that they have no conflicts of interest.

Ethical Approval This study used human glioma tissues and brain injury tissues obtained from Tiantan Hospital (Beijing, China). All procedures performed in studies involving human participants were in accordance with the Ethical Standards of the Institutional and/or National Research Committee and with the 1964 Helsinki Declaration and its later amendments or comparable ethical standards. All applicable international, national, and/or institutional guidelines for the care and use of animals were followed.

References

Altman BJ, Stine ZE, Dang CV (2016) From Krebs to clinic: glutamine metabolism to cancer therapy. Nat Rev Cancer 16:619–634

Biggs III WH, Meisenhelder J, Hunter T, Cavenee WK, Arden KC (1999) Protein kinase B/Akt-mediated phosphorylation promotes nuclear exclusion of the winged helix transcription factor FKHR1. Proc Natl Acad Sci USA 96:7421–7426

Cairns RA, Harris I, McCracken S, Mak TW (2011a) Cancer cell metabolism. Cold Spring Harb Symp Quant Biol 76:299–311

Cairns RA, Harris IS, Mak TW (2011b) Regulation of cancer cell metabolism. Nat Rev Cancer 11:85–95

Cantor JR, Sabatini DM (2012) Cancer cell metabolism: one hallmark, many faces. Cancer Discov 2:881–898

Choe G, Horvath S, Cloughesy TF, Crosby K, Seligson D, Palotie A, Inge L, Smith BL, Sawyers CL, Mischel PS (2003) Analysis of the phosphatidylinositol 30-kinase signaling pathway in GBM patients *in vivo*. Cancer Res 63:2742–2746

Christofk HR, Vander Heiden MG, Wu N, Asara JM, Cantley LC (2008) Pyruvate kinase M2 is a phosphotyrosine-binding protein. Nature 452:181–186

Dang CV (2012) Links between metabolism and cancer. Genes Dev 26:877–890

Dang CV, Le A, Gao P (2009) MYC-induced cancer cell energy metabolism and therapeutic opportunities. Clin Cancer Res 15:6479–6483

DeBerardinis RJ, Cheng T (2010) Q's next: the diverse functions of glutamine in metabolism, cell biology and cancer. Oncogene 29:313–324

DeBerardinis RJ, Mancuso A, Daikhin E, Nissim I, Yudkoff M, Wehrli S et al (2007) Beyond aerobic glycolysis: transformed cells can engage in glutamine metabolism that exceeds the requirement for protein and nucleotide synthesis. Proc Natl Acad Sci USA 104:19345–19350

DeBerardinis RJ, Lum JJ, Hatzivassiliou G, Thompson CB (2008) The biology of cancer: metabolic reprogramming fuels cell growth and proliferation. Cell Metab 7:11–20

DeHaven JE, Robinson KA, Nelson BA, Buse MG (2001) A novel variant of glutamine: fructose-6-phosphate amidotransferase-1 (GFAT1) mRNA is selectively expressed in striated muscle. Diabetes 50:2419–2424

Faubert B, Boily G, Izreig S, Griss T, Samborska B, Dong Z, Dupuy F, Chambers C, Fuerth BJ, Viollet B et al (2013) AMPK is a negative regulator of the Warburg effect and suppresses tumor growth *in vivo*. Cell Metab 17:113–124

Gan B, Lim C, Chu G, Hua S, Ding Z, Collins M, Hu J, Jiang S, Fletcher-Sananikone E, Zhuang L et al (2010) FoxOs enforce a progression checkpoint to constrain MTORC1-activated renal tumorigenesis. Cancer Cell 18:472–484

Gao P, Tchernyshyov I, Chang TC et al (2009) C-MYC suppression of miR23a/b enhances mitochondrial glutaminase expression and glutamine metabolism. Nature 458:762–765

Guertin DA, Stevens DM, Thoreen CC, Burds AA, Kalaany NY, Moffat J, Brown M, Fitzgerald KJ, Sabatini DM (2006) Ablation in mice of the MTORC components raptor, rictor, or mLST8 reveals that MTORC2 is required for signaling to Akt-FOXO and PKCalpha, but not S6K1. Dev Cell 11:859–871

Hagiwara A, Cornu M, Cybulski N, Polak P, Betz C, Trapani F, Terracciano L, Heim MH, Rüegg MA, Hall MN (2012) Hepatic MTORC2 activates glycolysis and lipogenesis through Akt, glucokinase, and SREBP1c. Cell Metab 15:725–738

Hosios AM, Hecht VC, Danai LV, Johnson MO, Rathmell JC, Steinhauser ML et al (2016) Amino acids rather than glucose account for the majority of cell mass in proliferating mammalian cells. Dev Cell 36:540–549

Hu Y, Riesland L, Paterson AJ, Kudlow JE (2004) Phosphorylation of mouse glutamine-fructose-6-phosphate amidotransferase 2 (GFAT2) by cAMP-dependent protein kinase increases the enzyme activity. J Biol Chem 279:29988–29993

Hudson CC, Liu M, Chiang GG, Otterness DM, Loomis DC, Kaper F, Giaccia AJ, Abraham RT (2002) Regulation of hypoxia-inducible factor 1alpha expression and function by the mammalian target of rapamycin. Mol Cell Biol 22:7004–7014

Kaelin WG Jr, Ratcliffe PJ (2008) Oxygen sensing by metazoans: the central role of the HIF hydroxylase pathway. Mol Cell 30:393–402

Kleszcz R, Paluszczak J, Krajka-Kuźniak V, Baer-Dubowska W (2018) The inhibition of C-MYC transcription factor modulates the expression of glycolytic and glutaminolytic enzymes in FaDu hypopharyngeal carcinoma cells. Adv Clin Exp Med 27:735–742

Koppenol WH, Bounds PL, Dang CV (2011) Otto Warburg's contributions to current concepts of cancer metabolism. Nat Rev Cancer 11:325–337

Le A, Lane AN, Hamaker M, Bose S, Gouw A, Barbi J et al (2012) Glucose-independent glutamine metabolism via TCA cycling for proliferation and survival in B cells. Cell Metab 15:110–121

Lee M, Theodoropoulou M, Graw J, Roncaroli F, Zatelli MC, Pellegata NS (2011) Levels of p27 sensitize to dual PI3K/mTOR inhibition. Mol Cancer Ther 10:1450–1459

Levine AJ, Puzio-Kuter AM (2010) The control of the metabolic switch in cancers by oncogenes and tumor suppressor genes. Science 330:134001344

Lunt SY, Vander Heiden MG (2011) Aerobic glycolysis: meeting the metabolic requirements of cell proliferation. Annu Rev Cell Dev Biol 27:441–464

Marroquin LD, Hynes J, Dykens JA, Jamieson JD, Will Y (2007) Circumventing the Crabtree effect: replacing media glucose with galactose increases susceptibility of HepG2 cells to mitochondrial toxicants. Toxicol Sci 97:539–547

Matsui Y, Lai ZC (2019) Bimolecular fluorescence complementation (BiFC) in tissue culture and in developing tissues of *Drosophila* to study protein–protein interactions. Methods Mol Biol 1893:75–85

Medina MA, Núñez de Castro I (1990) Glutaminolysis and glycolysis interactions in proliferant cells. Int J Biochem 22:681–683

Muellner MK, Uras IZ, Gapp BV, Kerzendorfer C, Smida M, Lechtermann H, Craig-Mueller N, Colinge J, Duernberger G, Nijman SM (2011) A chemical-genetic screen reveals a mechanism of resistance to PI3K inhibitors in cancer. Nat Chem Biol 7:787–793

Niimi M, Ogawara T, Yamashita T, Yamamoto Y, Ueyama A, Kambe T et al (2001) Identification of GFAT1-L, a novel splice variant of human glutamine: fructose-6-phosphate amidotransferase (GFAT1) that is expressed abundantly in skeletal muscle. J Hum Genet 46:566–571

Oki T, Yamazaki K, Kuromitsu J, Okada M, Tanaka I (1999) cDNA cloning and mapping of a novel subtype of glutamine:fructose-6-phosphate amidotransferase (GFAT2) in human and mouse. Genomics 57:227–234

Pelicano H, Martin DS, Xu RH, Huang P (2006) Glycolysis inhibition for anticancer treatment. Oncogene 25:4633–4646

Plas DR, Thompson CB (2005) Akt-dependent transformation: there is more to growth than just surviving. Oncogene 24:7435–7442

Qie S, Liang D, Yin C, Gu W, Meng M, Wang C et al (2012) Glutamine depletion and glucose depletion trigger growth inhibition via distinctive gene expression reprogramming. Cell Cycle 11:3679–3690

Rohle D, Popovici-Muller J, Palaskas N, Turcan S, Grommes C, Campos C, Tsoi J, Clark O, Oldrini B, Komisopoulou E et al (2013) An inhibitor of mutant IDH1 delays growth and promotes differentiation of glioma cells. Science 340:626–630

Shanware NP, Mullen AR, DeBerardinis RJ, Abraham RT (2011) Glutamine: pleiotropic roles in tumor growth and stress resistance. J Mol Med (Berl) 89:229–236

Tanaka K, Babic I, Nathanson D, Akhavan D, Guo D, Gini B, Dang J, Zhu S, Yang H, De Jesus J et al (2011) Oncogenic EGFR signaling activates an MTORC2-NF-kB pathway that promotes chemotherapy resistance. Cancer Discov 1:524–538

Tong X, Zhao F, Thompson CB (2009) The molecular determinants of de novo nucleotide biosynthesis in cancer cells. Curr Opin Genet Dev 19:32–37

Vadla R, Haldar D (2018) Mammalian target of rapamycin complex 2 (MTORC2) controls glycolytic gene expression by regulating Histone H3 Lysine 56 acetylation. Cell Cycle 17:110–123

Vander Heiden MG, Cantley LC, Thompson CB (2009) Understanding the Warburg effect: the metabolic requirements of cell proliferation. Science 324:1029–1033

Vyas B, Silakari O, Bahia MS, Singh B (2013) Glutamine: fructose-6-phosphate amidotransferase (GFAT): homology modelling and designing of new inhibitors using pharmacophore and docking based hierarchical virtual screening protocol. SAR QSAR Environ Res 24:733–752

Wang B, Moya N, Niessen S, Hoover H, Mihaylova MM, Shaw RJ, Yates JR III, Fischer WH, Thomas JB, Montminy M (2011) A hormone-dependent module regulating energy balance. Cell 145:596–606

Wang QS, Kong PZ, Li XQ, Yang F, Feng YM (2015) FOXF2 deficiency promotes epithelial-mesenchymal transition and metastasis of basal-like breast cancer. Breast Cancer Res 17:30

Warburg O (1956) On the origin of cancer cells. Science 123:309–314

Ward PS, Thompson CB (2012) Metabolic reprogramming: a cancer hallmark even Warburg did not anticipate. Cancer Cell 21:297–308

Wellen KE, Lu C, Mancuso A, Lemons JM, Ryczko M, Dennis JW et al (2010) The hexosamine biosynthetic pathway couples growth factor-induced glutamine uptake to glucose metabolism. Genes Dev 24:2784–2799

Wise DR, DeBerardinis RJ, Mancuso A et al (2008) Myc regulates a transcriptional program that stimulates mitochondrial glutaminolysis and leads to glutamine addiction. Proc Natl Acad Sci USA 105:18782–18787

Wise DR, Thompson CB (2010) Glutamine addiction: a new therapeutic target in cancer. Trends Biochem Sci 35:427–433

Yang C, Peng P, Li L, Shao M, Zhao J, Wang L, Duan F, Song S, Wu H, Zhang J, Zhao R, Jia D, Zhang M, Wu W, Li C, Rong Y, Zhang L, Ruan Y, Gu J (2016) High expression of GFAT1 predicts poor prognosis in patients with pancreatic cancer. Sci Rep 6:39044